Analytical Biochemistry **290,** 214–220 (2001)
doi:10.1006/abio.2001.4991, available online at http://www.idealibrary.com on IDEAL®

Miniaturization of a Hepatitis C Virus RNA Polymerase Assay Using a −102°C Cooled CCD Camera-Based Imaging System

Wei Zheng,*[,1] Steven S. Carroll,† James Inglese,* Robert Graves,‡ Leighton Howells,‡ and Berta Strulovici*

**Department of Automated Biotechnology, Merck & Company, 502 Louise Lane, North Wales, Pennsylvania 19454; †Department of Antiviral Research, Merck & Company, P.O. Box 4, West Point, Pennsylvania 19486; and ‡Amersham Pharmacia Biotech Inc., 800 Centennial Avenue, P.O. Box 1327, Piscataway, New Jersey 08855*

Received September 22, 2000; published online February 15, 2001

Innovations in detection technologies have allowed us to develop a novel assay in 1536-well plate format and assess the advantages of screen miniaturization compared with conventional high-throughput compound screening in 96- or 384-well plates. An HCV RNA polymerase assay has been miniaturized in 1536-well plates by using a new detection technology known as LEADseeker homogeneous imaging system. It uses a −102°C cooled charge-coupled device (CCD) camera and newly designed scintillation proximity microparticles. The miniaturized assay used europium-doped streptavidin-coated yttrium oxide (YO_x) or polystyrene (PS) microspheres to capture biotin-labeled [^{3}H]RNA product transcripts. Beads in proximity to the radioisotope convert the emitted β^- particles into photons having wavelengths in the red region of the visible spectrum, optimal for detection by the CCD camera. Because the camera collects light from all wells of the plate simultaneously, 1536-well plates are imaged as rapidly as 384-well plates, on the order of 10 min per plate. The assay has a signal to background of approximately 20-fold, satisfactory for high-throughput robotics screening. The enzyme kinetics and potency of a known inhibitor were similar to those obtained from the conventional assay using scintillation proximity assay (SPA) beads and a scintillation plate counter. Furthermore, the newly developed microbeads (emitting at 610 to 620 nm) are less prone to quenching effects caused by yellow-colored compounds, than conventional SPA beads or scintillation fluid (emitting at 400 to 480 nm region). Thus, the LEADseeker imaging system is a useful new tool for miniaturization of assays for high-throughput screening. © 2001 Academic Press

Key Words: **miniaturization; high-throughput screening; HCV RNA polymerase; CCD imaging system.**

Recent advances in human genomics and combinatorial chemistry technologies are predicted to provide new opportunities for lead identification in an increasing number of therapeutic areas (1–3). A major challenge to our ability to capitalize on these breakthroughs in a timely manner is reagent availability, which can be solved by emerging miniaturization technologies. Screen miniaturization, as defined by an ability to perform assays in less then 10 μl volume and with high speed, is contingent on appropriate pipetting devices (4), the availability of a variety of higher density well microtiter plates, as well as ultrasensitive, versatile, and fast detection systems. This last point will be the focus of this report.

In the past 5 years, the development of fluorescence resonance energy transfer (FRET)[2] and SPA-based screening technologies enabled the move toward nonseparation screening assay formats (5, 6), amenable to screen miniaturization. Although FRET-based assays have been adopted in many assay types, the radioisotope-based SPA remains at present a popular choice for

[1] To whom correspondence and reprint requests should be addressed. Fax: 215-993-3625. E-mail: wei_zheng@merck.com.

[2] Abbreviations used: CCD, charge-coupled device; YO_x, yttrium oxide; PS, polystyrene; SPA, scintillation proximity assay; FRET, fluorescence resonance energy transfer; HCV, hepatitis C virus; PVT, poly(vinyl toluene).

0003-2697/01 $35.00

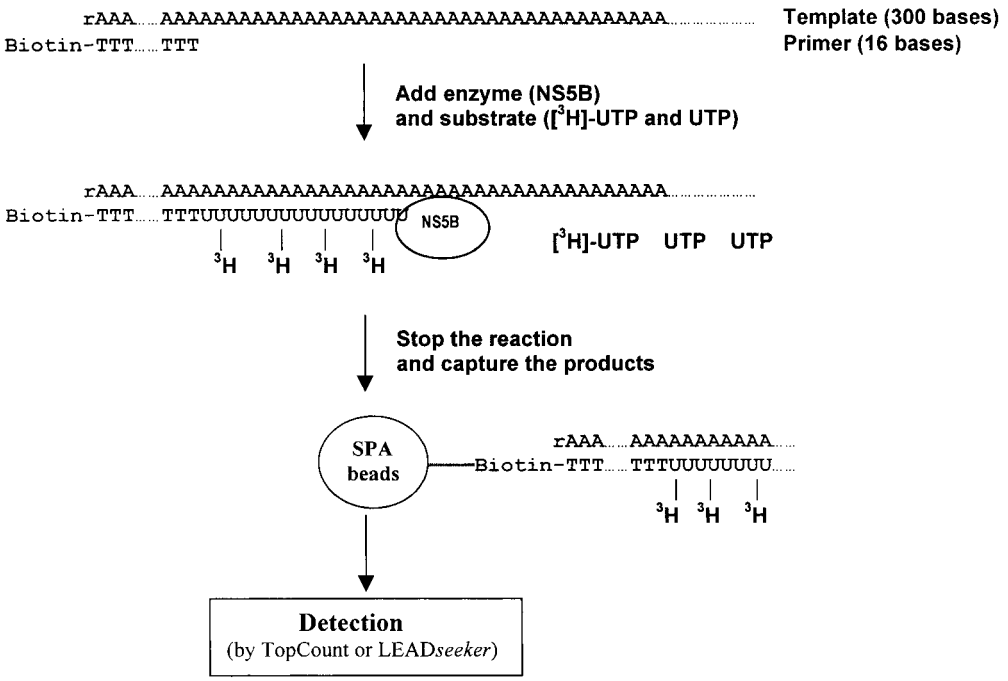

FIG. 1. Schematic diagram of an RNA polymerase assay. The newly transcribed RNAs were captured on streptavidin-coupled beads and detected by either counting with a PMT-based or CCD camera-based system.

assay miniaturization, due to its high sensitivity and broad applicability.

Traditionally, radioactivity has been detected by photomultiplier tube-based scintillation counting, a process having high sensitivity and signal:background ratio, two critical parameters for quality screening assays. A limiting factor, however, has been the sample counting time. Due to the low number of photons emitted in a short time interval, each sample is usually counted for 1 min to obtain reliable results. Therefore, when using a plate counter with 12-photomultiplier tubes such as the commercially available TopCount (Packard) or MicroBeta (Wallac), the plate counting time is 10 min (1 min/well) for a 96-well plate, or up to 40 min for a 384-well plate. Another disadvantage of the photomultiplier tube-based scintillation counting is that the sensitivity of detection is proportionally decreased as the assay volume is reduced, which precludes a significant reduction in reagent consumption without a loss in signal. Therefore, screen miniaturization is difficult in the scintillation counting environment using the existing technology, which is also limited to 96- and 384-well plates.

LEADseeker, a CCD-based detection system (7, 8), emerged recently as a sensitive and rapid instrument for measuring radioisotope activity in a field format and thus capable of handling plate formats having 96-, 384-, or 1536-wells/plate. The CCD chip is cooled to −102°C to greatly reduce dark current noise arising from thermal fluctuations at higher temperatures, while software algorithms correct for cosmic events that can create "false" signals. A specially designed telecentric Borealis lens eliminates the parallax effect or "shadowing" that occurs when imaging the peripheral wells of microtiter plates using standard lenses. Because the CCD chip is most sensitive to light in the red region of the spectrum, newly designed microspheres based on europium-doped PS or YO_x having an emission peak at 615 nm allow the development of non-separation SPAs using LEADseeker.

The experiments described here were designed to miniaturize the HCV RNA polymerase assay using a SPA format for the detection of reaction products. Over 170 million people worldwide are currently infected by hepatitis C virus (HCV). More than 50% of acute HCV infections eventually develop into a chronic disease, which may lead to liver cirrhosis and hepatocellular carcinoma. Interferon-α is the most frequently used therapeutic agent to treat HCV infection but less than 20% of patients respond to the therapy (9). New treatments are clearly needed to combat the HCV infection. The RNA-dependent RNA polymerase of HCV is an attractive target for drug development since it plays a critical role in the replication of the viral genome (10).

MATERIALS AND METHODS

Materials. HCV RNA polymerase (NS5B) was expressed in *Escherichia coli* and purified to >90% purity (11). [^{3}H]UTP, UTP, streptavidin-coupled poly(vinyl

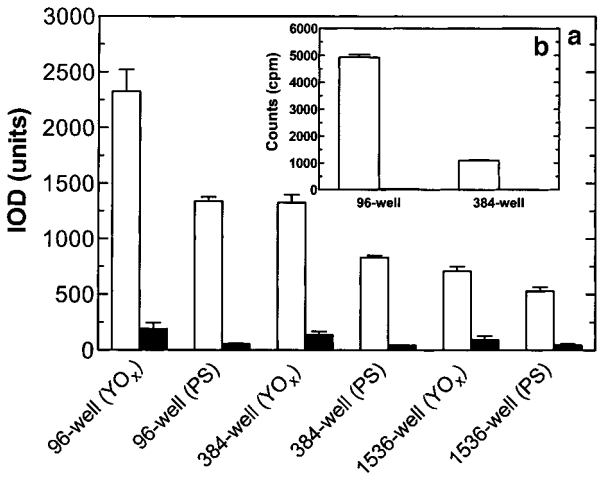

FIG. 2. (a) Detection of HCV RNA polymerase product in 96-, 384-, and 1536-well plates using the LEADseeker imager. Total signal and background of the HCV RNA polymerase SPA assay were measured with 30 nM enzyme and 1 μM [^{3}H]UTP using yttrium oxide (YO_x) or polystyrene (PS) imaging beads and LEADseeker imager for detection. Each plate was counted for 10 min. The signal/background ratio in the assay using YO_x imaging beads was 28, 14, and 20 for 96-, 384-, and 1536-well plates, respectively. In the assay using PS imaging beads, the signal/background ratio was 26, 21, and 18 for 96-, 384-, and 1536-well plates, respectively. Open bars are total signal and closed bars are background. Each bar represents the average of four measurements. Error bars are standard deviation. (b) Comparison of signal/background in 96- and 384-well plates using a TopCount plate reader. Total signal and background of the HCV RNA polymerase SPA assay were determined with 30 nM enzyme and 1 μM [^{3}H]UTP) using poly(vinyl toluene) (PVT) beads for product capture and TopCount for signal detection. The counting time was 1 min per well. The signal/background ratio was 103-fold in the 96-well plate assay and 46-fold in the 384-well plate assay. Open bars are total signal and solid bars are background. Each bar represents the average of eight measurements. Error bar is standard deviation.

toluene) SPA beads (PVT beads), streptavidin-coupled yttrium oxide (YO_x) and polystyrene (PS) imaging beads were obtained from Amersham Pharmacia Biotech. The assay buffer contained 10 mM KCl, 20 mM Tris–HCl, pH 7.5, 2 mM $MgCl_2$, 5 mM DTT and 0.01% Triton X-100 (reagents purchased from Sigma). The 96- and 384-well solid white plates were purchased from

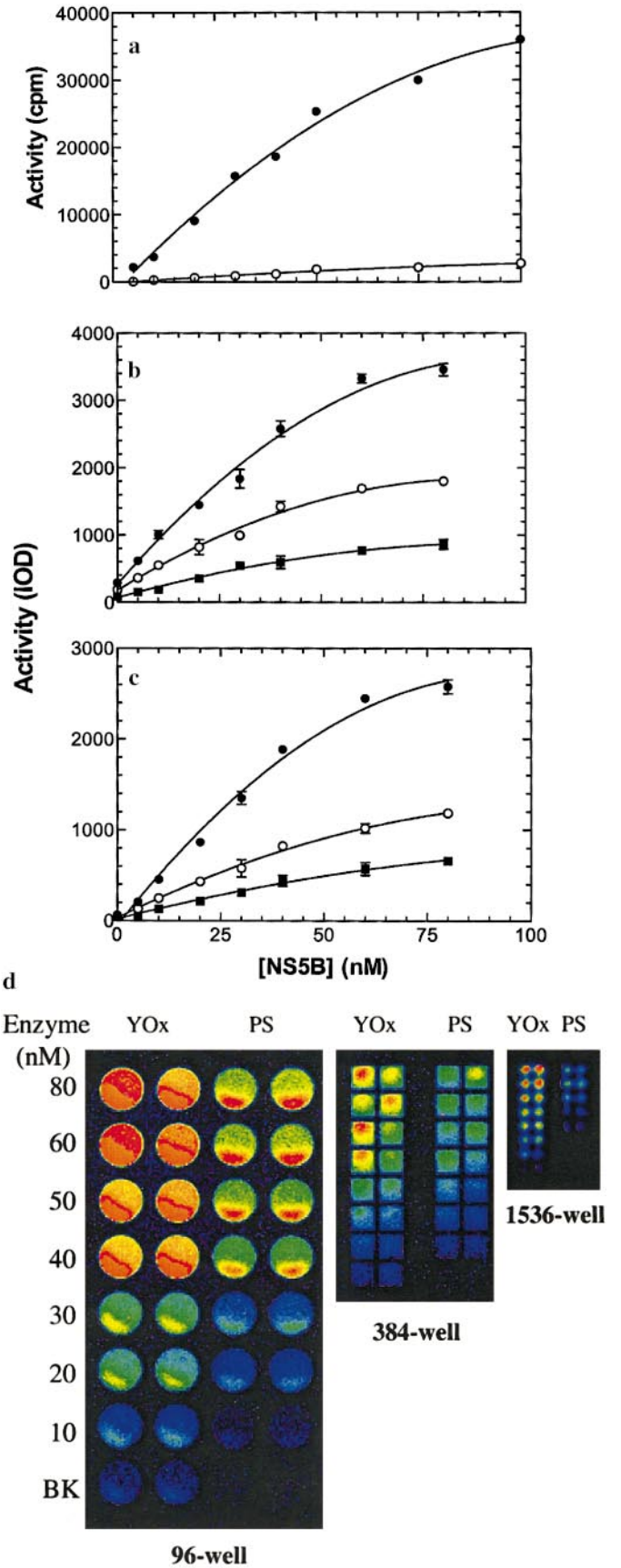

FIG. 3. Concentration responses of the HCV RNA polymerase (NS5B) determined by either PMT- or CCD-based detectors. (a) The 96-well (●) and 384-well (○) plates with PVT beads were counted by a TopCount. (b) The 96-well (●), 384-well (○), and 1536-well plate (■) with YO_x beads were detected by LEADseeker imaging system. (c) The 96-well (●), 384-well (○), and 1536-well plate (■) with PS beads were detected by LEADseeker imaging system. The concentration of 30 nM enzyme was used in all other experiments. (d) Pseudocolor images of the concentration response of the HCV RNA polymerase acquired by the LEADseeker imaging system from the same plates of which the data were described in b and c. Each point in the curves is the mean of four measurements and the error bars are the standard deviation.

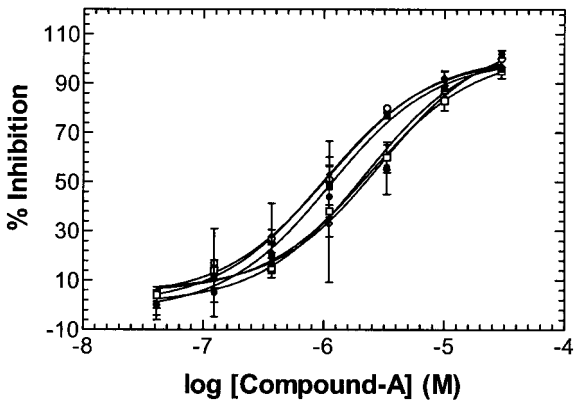

FIG. 4. Inhibition of HCV RNA polymerase activity by compound A, a known inhibitor in the [^{3}H]-SPA assay determined by TopCount and LEADseeker imaging system (the IC_{50} values are 1 to 3 μM calculated from above curves). TopCount detection using PVT beads in a 60-μl assay, IC_{50} = 1.1 μM (■) or 15 μl assay volume, IC_{50} = 2.4 μM (□). LEADseeker detection using YO_x beads in a 15-μl assay, IC_{50} = 2.2 μM (●) or 6 μl assay volume, IC_{50} = 1.1 μM (○). LEADseeker detection using PS beads in a 15-μl assay, IC_{50} = 0.99 μM (◆) or a 6-μl assay volume, IC_{50} = 2.4 μM (◇). Each point in the curves is the means of four measurements and the error bars are the standard deviation.

Corning Costar. The 1536-well solid white plates having a 12-μl volume capacity per well were obtained from Greiner.

Instruments. LEADseeker (Amersham Pharmacia Biotech), a CCD-camera-based imaging system, was used to determine the radioisotope signal from YO_x and PS beads in 96-, 384-, and 1536-well plates. Topcount (Packard Instruments), a plate scintillation counter equipped with 12 photo multiplier tubes (PMTs), was used to count the radioisotope signal from PVT SPA beads in 96- and 384-well plates. All liquid dispensing in this study was performed manually using BioHit proline single channel electronic pipettors (Vangard).

HCV polymerase assay. HCV RNA polymerase catalyzes the incorporation of radiolabeled uridine triphosphate into a primer-template substrate composed of biotinylated-oligo$(dT)_{16}$ hybridized to polyriboadenosine. After quenching the reaction by the addition of EDTA which chelates the required Mg^{2+}, the product is captured onto streptavidin-coated SPA beads.

The poly(A) template (300 bases) and oligo(dT) primer (16 bases) were preannealed by incubation at room temperature for 60 min at a 1:1 ratio. The assay was performed essentially as described by Carroll *et al.* (11). Briefly, as described in Fig. 1, 20 μl/well purified HCV RNA polymerase (NS5B) and primer/template mixture, 20 μl/well compound solution or assay buffer, and 20 μl/well [^{3}H]UTP substrate were added to a 96-well plate and incubated at 30°C for 60 min. The final concentrations were 30 nM NS5B, 20 nM primer/template and 1 μM [^{3}H]UTP (0.35 μCi/well in 96-well plate assay). The reaction was terminated by addition of 30 μl/well 0.5 M EDTA with 0.2 mg streptavidin-coupled PVT, YO_x, or PS beads except in the experiment for the enzyme–concentration curves where 0.4-mg beads were added. The plate was counted for 1 min/well in a TopCount plate reader (10 min/plate for a 96-well plate, or 40 min/plate for a 384-well plate) or 10 min/plate in a LEADseeker imaging system for any density of plate.

The total assay volumes were proportionally reduced from 60 μl in 96-well plates to 15 and 6 μl for 384-well and 1536-well plates, respectively. Therefore, the final concentrations of all reagents including enzyme and substrate remained constant regardless of assay volume. The radioactivity was 0.0875 and 0.035 μCi/well for 384- and 1536-well plates, respectively. The amount of streptavidin-coated beads was reduced to 0.05 mg/well for a 384-well plate and to 0.02 mg/well for 1536-well plate.

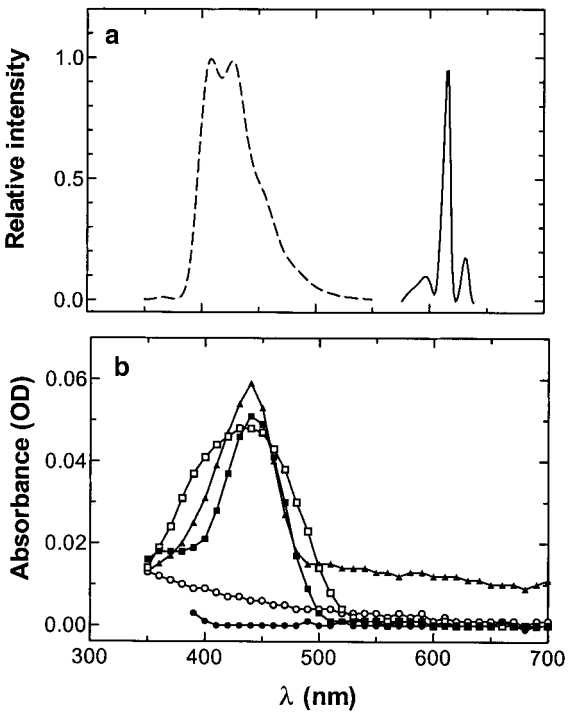

FIG. 5. Comparison of emission spectrum of PVT and YO_x beads with the absorbance spectrum of compounds. (a) PVT beads emit between 400 to 480 nm (dashed line) while YO_x beads emit at 610–620 nm (solid line). (b) Yellow-colored compounds: Compound 1 (■), compound 2 (□), and compound 4 (▲) have similar absorbance peaks from 400 to 500 nm. The match between the emission spectrum of the regular SPA beads with the absorbance spectrum of yellow-colored compounds results in a color quench of the signal and can produces false positive during screening. Compound A, a known inhibitor (●), and compound 3 (○), both colorless, showed no significant absorbance from 400 to 750 nm. The data are the means of two measurements.

RESULTS AND DISCUSSION

Signal and background of the HCV RNA polymerase assay detected by scintillation counting (PMT-based) and by imaging technology (CCD camera-based) in 96-, 384-, and 1536-well plate formats. The total signal and background of the HCV RNA polymerase assay were determined using 30 nM enzyme, 20 nM primer/template and 1 μM [^{3}H]UTP (0.35, 0.875, and 0.035 μCi/well, respectively, for 96-, 384-, and 1536-well plates). The assay volume was proportionally reduced in higher density plate format (60, 15, and 6 μl for 96-, 384-, and 1536-well plates, respectively). The initial enzyme reaction was the same for both the SPA and LEADseeker-based assay formats except for different types of streptavidin-coupled beads used to capture the biotin-linked product after termination of the enzyme reaction.

In experiments using PMT-compatible PVT beads for capturing the ^{3}H product, the total signal was proportional to the assay volume. Approximately 22% ($\pm$1%) of the signal was observed for a 15-μl assay in a 384-well plate, compared to that in a 60-μl assay in a 96-well plate (Fig. 2b). However, the counting time increased with the higher density plates from 10 min/96-well plate to 40 min/384-well plate. Therefore, although reducing reagent consumption by three-fold, the 384-well format results in a fourfold increase in counting time. This bottleneck, i.e., excessive counting time in high-density well plate format, would be effectively removed by using CCD camera-based instruments that are not restricted by plate geometry and that image an entire plate at once.

With the LEADseeker, we assessed signal amplitude, as well as signal to noise ratios using YO_x or PS imaging beads, while varying the assay volume and the plate density, from 96-, to 384-, to 1536-well plate formats (Fig. 2a). The signal amplitude was twofold higher using YO_x beads than for PS beads, although the assay background (noise) was also slightly higher. The signal measured from 384-well plate assays having 15-μl assay volumes was 56% ($\pm$6.4%) and 61% ($\pm$3.1%) of that in 96-well plate assays, using YO_x and PS beads, respectively. In a 1536-well plate using YO_x beads and PS beads, the signal was 29% ($\pm$3.8%) and 38% ($\pm$3.9%), respectively, of that in a 96-well plate, although the assay volume decreased 10-fold in the 1536-well plate assay (6 μl assay volume). Therefore, the signal detected by a CCD-based imaging system did *not* proportionally decrease with a *reduction* in assay volume and total radiolabel as assays moved into higher density plates. This improved light collection characteristic arises from the smaller surface-to-volume ratio of a 1536-well plate which effectively concentrates light emission into a smaller area. This phenomenon has also been observed and explained elsewhere (7) which benefits assay miniaturization, permitting the scaling down of assays, while maintaining sufficient signal for detection.

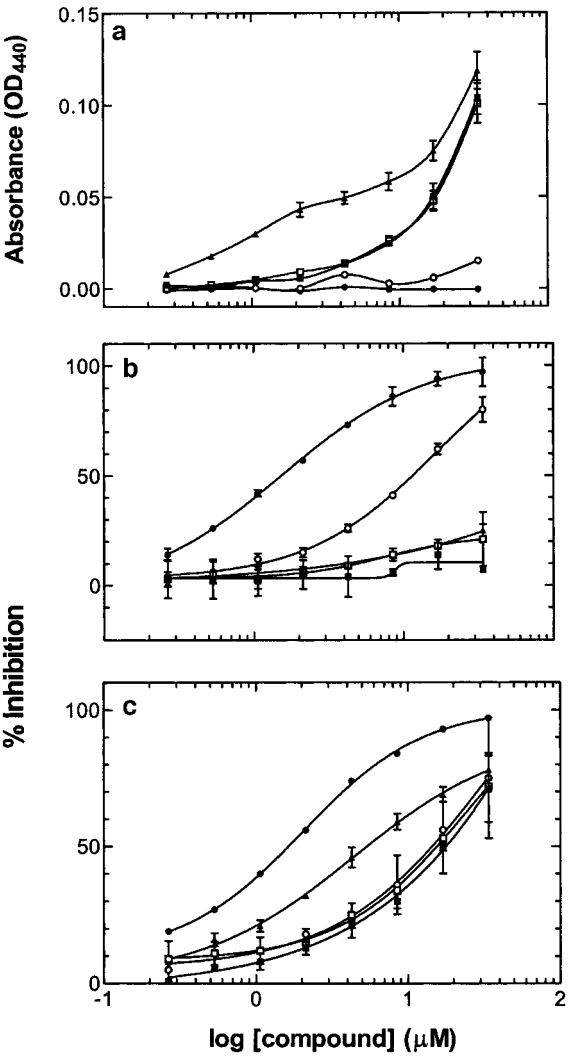

FIG. 6. Comparison of the inhibitory effect of compounds on the HCV RNA polymerase activity determined using regular SPA beads and LEADseeker beads with the absorbance of the compounds at 440 nm. (a) The EC_{50} value for absorbance at 440 nm was 8 μM for compound 4 (▲) and 11 μM for compound 1 (■) and compound 2 (□). Compound A, a known inhibitor (●), and compound 4 (○), both colorless, showed no significant absorbance at 440 nm. (b) The IC_{50} value was 1.5 μM for compound A (●) and 10.2 μM for the colorless compound 3 (▲). Three yellow-colored compounds, compounds 1, 2, and 4, were not active at concentrations up to 30 μM with detection of product using LEADseeker beads. (c) The IC_{50} value was 1.6 μM for compound A (●) and 6.1 μM for the colorless compound 3 (▲) with detection of product using the regular SPA beads. Three yellow-colored compounds had IC_{50} values around 10.3 μM with detection of product using the regular SPA beads. Each point in the curves is the mean of four measurements and the error bars are the standard deviation.

TABLE 1

Comparison of the Inhibitory Effect of Compounds on the HCV RNA Polymerase Activity in Regular SPA Beads and LEADseeker Beads with the Absorbance of Compounds at 440 nm

Compound	Compound color	EC_{50} (μM) in absorbance (440 nm)	IC_{50} (μM) in regular SPA beads	IC_{50} (μM) in LEADseeker beads
1	Yellow	8.1	10.4	Not active
2	Yellow	11.2	10.3	Not active
3	Colorless	Not active	6.3	10.2
4	Yellow	11.1	10.2	Not active
A (known inhibitor)	Colorless	Not active	1.6	1.5

Concentration response of HCV RNA polymerase determined by PMT-based scintillation counting and CCD camera-based imaging in 96-, 384-, and 1536-well plates. To further assess the suitability of the CCD camera-based imaging technology for assaying the activity of the HCV RNA polymerase, an enzyme concentration–response experiment was performed in the three types of microtiter plates. The enzyme concentration–response curves were similar across the three types of the plates, bead type, and detection methods (Figs. 3a–3c). Substrate K_m values remained the same in these experiments as well (data not shown here). Figure 3d shows the pseudocolor images acquired by the LEADseeker imaging system from which the data in Figs. 3b and 3c were derived. These results indicate that the LEADseeker imaging assay format for the HCV RNA polymerase assay produces results that are comparable with those obtained using conventional SPA format.

Comparison of the IC_{50} for an inhibitor of HCV RNA polymerase determined in conventional SPA scintillation counting and CCD-imaging assay formats. During the high-throughput screening performed in our laboratories using the SPA-based assay in the 96-well format on a fully automated robotics platform (Robolab with integrated TopCount), several classes of inhibitors have been identified (not shown). Here we assess the effect of compound A, a known inhibitor, on the polymerase activity using the miniaturized assay conditions established (Figs. 2 and 3). The IC_{50} of compound A was determined in an experiment using 30 nM HCV RNA polymerase and 1 μM [^{3}H]UTP as the substrate. The results (Fig. 4) demonstrated that the inhibition of RNA polymerase activity in the presence of compound A was similar in 96-, 384-, and 1536-well plates measured by either TopCount or LEADseeker imaging system.

Reduced color quenching with YO_x and PS beads compared to conventional SPA beads. Color quenching can be an issue in SPA using PMT-based scintillation counters. SPA beads emit light in the blue region of the spectrum (400 to 480 nm) which is quenched by yellow and brown compounds which are common in most compound libraries. Figure 5 shows that this effect of yellow-colored compounds did not occur with YO_x and PS beads used with imaging detection, due to a shift in the photon emission region (610 to 620 nm) for these beads. It is estimated that 5 to 15% of the compounds in a collection have yellow, brown, or red color. By contrast, blue-colored compounds, which would affect the assay with LEADseeker beads, are relatively rare in compound libraries. To determine if CCD-imaging using YO_x or PS beads would be less prone to false positives resulting from yellow-colored compounds, a group of five compounds including two colorless compounds (a known inhibitor and a potential "hit") and three yellow-colored compounds was tested in the HCV RNA polymerase assay. All five compounds appeared active in the conventional SPA assay when quench correction was not applied (Fig. 6c); however, only the two colorless compounds, the known inhibitor and compound 3, registered as active in the CCD-based imaging assay (Fig. 6b). The putative inhibitory activity of the three yellow-colored compounds in the SPA assay measured in a PMT-based instrument was caused by color quenching because their concentration-dependent absorbance at 440 nm (Fig. 6a) paralleled the IC_{50} curve measured by a SPA assay (Fig. 6c and Table 1). The lower susceptibility of YO_x and PS beads to color quenching would be advantageous to reducing "false positives" during screening of large compound collections.

CONCLUSIONS

Here we demonstrate the transferability of the HCV RNA polymerase assay from a conventional SPA-based assay in 96-well plate format to 1536-well plate format using the LEADseeker imager. There are obvious advantages to using a CCD-based detection system in a miniaturized assay format: (1) a 15-fold reduction in data acquisition time, (2) a 9-fold reduction in reagent usage, (3) a signal:background ratio of approximately 20-fold, acceptable for HTS, (4) enzyme kinetics and potency of a known inhibitor consistent with those determined in a standard 96-well plate assay, (5) the use of YO_x and PS LEADseeker beads to reduce the number of false posi-

tives caused by the quenching effect of yellow-colored compounds which would otherwise arise with conventional SPA beads, and (6) a significant reduction in the volume of radioactive waste for disposal.

To adapt this assay to a form suitable for HTS requires more than an advanced detection methodology. Liquid handling is a critical element in screen miniaturization as is the dispensation of beads into 1536-well plates with SPA-formatted assays. Due to the advantages of assay miniaturization demonstrated in this report, it is worthwhile to invest time and effort in the development of special instrumentation for reagent dispensing, in particular robotics-friendly instrumentation.

REFERENCES

1. Palfreyman, M. G. (1998) Functional genomics conference: From identifying proteins to faster drug discovery. *Expert Opin. Invest. Drugs* **7,** 1201–1207.
2. Gordon, E. M., Barrett, R. W., Dower, W. J., Fodor, S. P., and Gallop, M. A. (1994) Applications of combinatorial technologies to drug discovery. 2. Combinatorial organic synthesis, library screening strategies, and future directions. *J. Med. Chem.* **37,** 1385–1401.
3. Gordon, E. M., Gallop, M. A., and Patel, D. V. (1996) Strategy and tactics in combinatorial organic synthesis. Applications to drug discovery. *Acc. Chem. Res.* **29,** 144–154.
4. Rose, D. (1999) Microdispensing technologies in drug discovery. *Drug Discovery Today* **4,** 411–419.
5. Hart, H. E., and Greenwald, E. B. (1979) Scintillation proximity assay (SPA): A new method of immunoassay. Direct and inhibition mode detection with human albumin and rabbit antihuman albumin. *Mol. Immunol.* **16,** 265–267.
6. Tsien, R. Y., Bacskai, B. J., and Adams, R. (1993) FRET for studying intracellular signaling. *Trends Cell Biol.* **3,** 242–245.
7. Ramm, P. (1999) Imaging systems in assay screening. *Drug Discovery Today* **4,** 401–410.
8. Beveridge, M., Park, Y. W., Hermes, J., Marenghi, A., Brophy, G., and Santos, A. (2000) Detection of p56ick kinase activity using scintillation proximity assay in 384-well format and imaging proximity assay in 384- and 1536-well format. *J. Biomol. Screening* **5,** 205–211.
9. Clarke, B. (1997) Molecular virology of hepatitis C virus. *J. Gen. Virol.* **78,** 2397–2410.
10. Lohmann, V., Roos, A., Korner, F., Koch, J. O., and Bartenschlager, R. (1998) Biochemical and kinetic analyses of NS5B RNA-dependent RNA polymerase of the hepatitis C virus. *Virology* **249,** 108–118.
11. Carroll, S. S., Sardana, V., Yang, Z., Jacobs, A. R., Mizenko, C., Hall, D., Hill, H., Zugay-Murphy, J., and Kuo, L. C. (2000) Only a small fraction of purified hepatitis C RNA-dependent RNA polymerase is catalytically competent. *Biochemistry* **39,** 8243–8249.